

Original article

Transient temperature distribution on the corneal endothelium during ophthalmic phacoemulsification: a numerical simulation using the nodeless variable element

Wiroj Limtrakarn^a, Somporn Reepolmaha^b, Pramote Dechaumphai^c

^aDepartment of Mechanical Engineering, Faculty of Engineering, Thammasat University, Rungsit Campus, Pathumthani 12120; ^bDepartment of Ophthalmology, Faculty of Medicine, Srinakharinwirot University, Nakhonayok, 26120, Thailand; ^cDepartment of Mechanical Engineering, Faculty of Engineering, Chulalongkorn University, Bangkok 10330

Background: During cataract operation (phacoemulsification), a phaco needle-tip is inserted into the anterior chamber of eye. Then, heat is generated by the oscillation of the phaco needle, which may injury the corneal endothelial cells. There are no data available for temperature responses at the corneal endothelium to heat from the phaco needle during phacoemulsification.

Objective: Investigate temperature distribution on the corneal endothelium during ophthalmic phacoemulsification using numerical simulation, and compare the transient temperature response to heat between balanced salt solution (BSS) and ophthalmic viscoelastic device (OVD), Viscoat[®].

Methods: Heat flux from a phaco needle was measured with thermal properties of BSS and AVS in an experimental setting. Then, nodeless variable finite element method was applied to predict temperature changes in the eye by the phaco needle inserted into the anterior chamber. The transient temperature distribution on the corneal endothelium was calculated at 10, 20, and 30 seconds after heat generation by the needle.

Results: The heat generation of phaco needle without sleeve cover was 1.6 kW/m². The numerical simulation showed that the maximum temperature occurs on the wound location at all times after heat generation by the phaco needle. Especially, at time 30 seconds, it was 49.2 and 41.7°C in BSS and OVD, respectively. The temperature elevation by the phaco needle was lower in OVD than BSS.

Conclusion: Phacoemulsification is a heat-generating procedure performed between the anterior chamber structures of eye. During this procedure, OVD may protect the corneal endothelium against heat better than BSS.

Keywords: Balanced salt solution, corneal endothelial cell, nodeless variable element, numerical simulation, phacoemulsification, ophthalmic viscoelastic device

Cataract is the most common cause of blindness [1]. This is effectively confronted with by cataract operation called phaco-emulsification. The ophthalmic operation accounts for more than 80% of the ophthalmic field.

A well-known serious late complication of the operation is corneal blindness called pseudophakic bullous keratopathy (PBK). The PBK patient progressively suffers from many annoying symptoms such as irritating foreign body sensation in the affected eye, photophobia, tearing, and decreased vision due to corneal haze. As a result, PBK is the leading causes of corneal transplantation [2].

Corneal endothelial cells are an important non-regenerative corneal innermost layer to

Correspondence to: Dr. Wiroj Limtrakarn, Department of Mechanical Engineering, Faculty of Engineering, Thammasat University, Rungsit Campus, Pathumthani 12120, Thailand. E-mail: limwiroj@tu.ac.th

maintain corneal transparency processes. The corneal endothelial cells are often injured by phacoemulsification during the operation for PBK. Many factors are involved in the cell injury during the operation, including free radical, shock wave, and direct mechanical trauma [3, 4]. Thermal factor during such operation is also serious in the operative complication.

During ophthalmic phaco-emulsification, a surgeon-controlled oscillating phaco needle-tip is inserted into the anterior chamber to emulsify lens materials. The oscillation of phaco needle-tip is driven by the attached piezoelectric crystal at variable presented stroke length, at a certain frequency, i.e. 28.5 or 40 Hz (For a phaco needle-tip inserted in the eye, see Appendix). Then, heat is generated by the oscillation of the phaco needle. This heat generation has been directly examined using thermal cameras [5-8]. It has been demonstrated that phaco needle generates heat along its entire length. However, the heat responses have been limited by experiment. There is no data available for temperature changes on the corneal endothelium during ophthalmic phacoemulsification.

The corneal endothelium exists as a monolayer of cell at the innermost part of cornea. Heat collection from the phaco needle that is inserted may be responsible for corneal endothelial cell injury [9]. In fact, when the phaco needle tip is inserted is fully occluded by lens material fragment in the anterior chamber, biofluid or solution cannot flow in and out of the chamber while the oscillating phaco needle emulsifies the engaged lens fragment and generates heat. Therefore, the highest risk of heat-induced cell-injury occurs during this particular period and many

times during each operation.

In this paper, we simulated temperature changes in the eye chamber during performing phaco-emulsification. Based on heat transfer and two-dimensional (2D) finite element equation, computational procedure was carried out to predict the transient temperature distribution in the eye chamber. Defining two cases of phacoemulsification where the anterior chamber was fully filled by balanced salt solution (BSS) or ophthalmic viscoelastic device (OVD), we compared the transient temperature response at the corneal endothelium between BSS and OVD.

Methods

Experiment

The specific heat capacity and the thermal conductivity coefficient of BSS and OVD were tested using the differential scanning calorimeter (DSC) (Mettler-Toledo Inc, Columbus, USA) and hot disk thermal constants analyzer (TCA) (Hot Disk AB, Gothenburg, Sweden), respectively [10]. The TCA power started at 0.05 W for five seconds.

To measure the heat generation from a phaco needle, we used as shown in **Fig. 1**. The fluid media was distilled water. For heat generation, the Millennium[®] phaco machine (Bausch & Lomb Co, New York, USA) was used. During the experiment we get the piezoelectric crystals at its maximum power 400% phaco-power-setting a 160 micron stroke length. To measure the temperature on the phaco needle surface, the resistance temperature detector PT100 was used as a temperature sensor. The phaco needle was operated with and without sleeve cover.

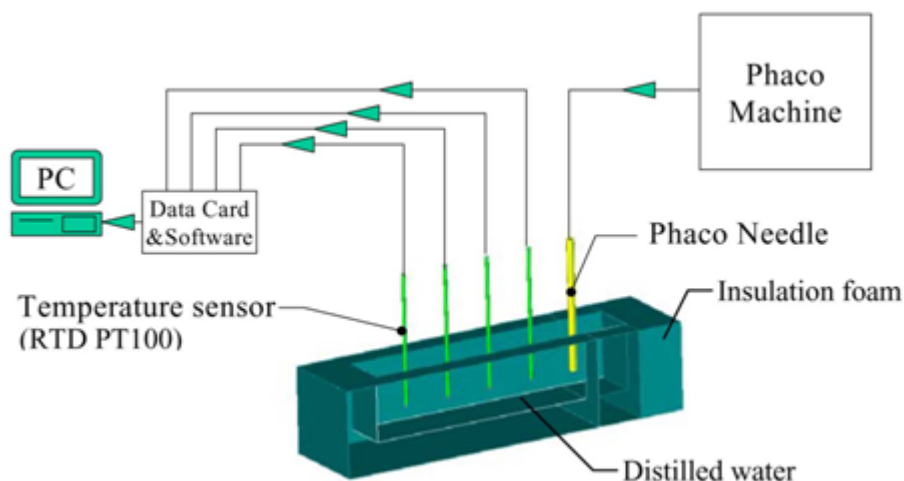


Fig. 1 Experimental set-up to measure heat generation from a phaco needle.

Numerical simulation

We investigated temperature changes on the median plane of eye where a phaco needle was inserted in the anterior chamber during performing phaco-emulsification. We assumed that temperature (T) in the eye obeys 2D transient heat transfer equation [11] and boundary conditions given by specified temperature, convection heat transfer, and specified heat flux, as shown in the Appendix.

In the numerical computation, we used element interpolation functions and finite element matrices [12-14] where triangular element consists of three nodes and three nodeless variables, as shown in Appendix. We drew a two-dimensional CAD (Computer-Aided Engineering) model to follow the ocular anatomy [15]. **Figure 2** shows the finite element model that was constructed with 9,311 elements.

Result

Thermal properties of BSS and AVS, and heat generation by the phaco needle

Table 1 shows the measured specific heat capacity and thermal conductivity coefficient of BSS and OVD.

Transient temperature distribution by simulation

In the numerical simulation, heat generation (q_g) from the phaco needle was assumed to be the heat flux of 1.6 kW/m². Temperature (T_∞) at the outer surface of the cornea was assumed to be the room temperature (25°C). The anterior chamber was fully filled with BSS or OVD. Using their thermal properties measured (**Table 1**), we calculated the thermal diffusivity ($k/\rho c$; k: thermal conductivity coefficient, ρ : density, c: specific heat capacity) as follows:
 2.36 x10⁻⁰⁹ (m²/sec) for BSS,
 1.19 x10⁻⁰⁸ (m²/sec) for OVD.

These values were used for solving the finite element equations. For the thermal properties of eye, we used those employed by Cichelki [16].

Figure 3 shows the temperature response using BSS at the time of 30 seconds.

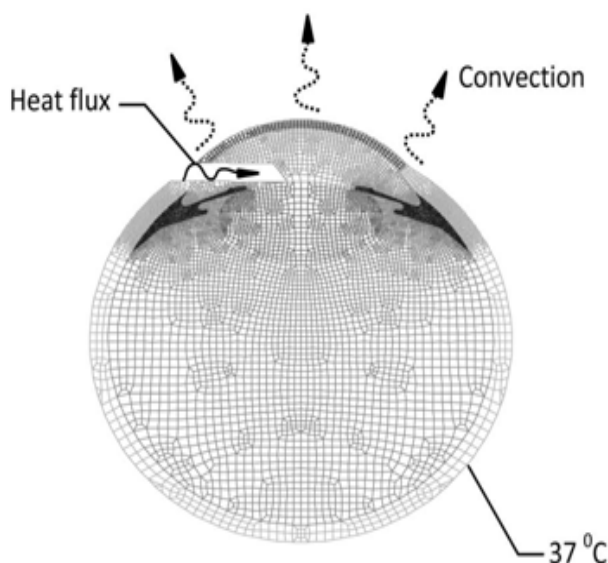


Fig. 2 Finite element model of eye.

Table 1. Specific heat capacity and thermal conductivity coefficient of BSS and AVS.

Solution	Specific heat capacity (J/gK)	Thermal conductivity coefficient (W/mK)
Balance salt solution (BSS)	2.45	0.65
Alcon viscoat solution (OVD)	3.91	0.47

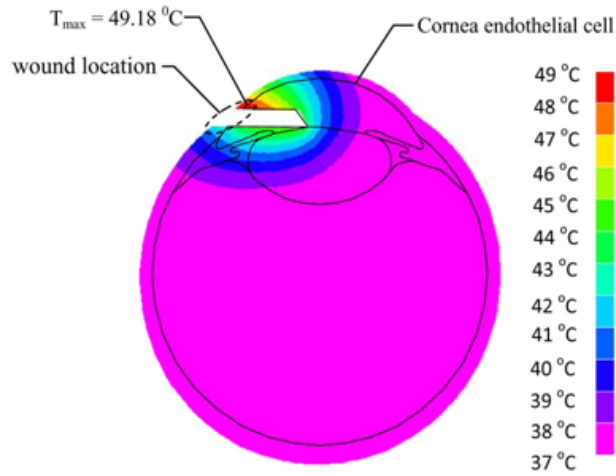


Fig. 3 Temperature distribution in eye 30 seconds after insertion of the needle.

With initial temperature of 37°C at $t=0$, the transient temperature response at the time of 30 seconds was computed. The time-interval required for this computation was approximately 0.1 second. Figure 4 shows the transient temperature response plotted along inner corneal surface at 10, 20, and 30 seconds for BSS and OVD. Interestingly, the computed temperature on the corneal endothelium

was lower in OVD than in BSS at any time and location. The maximum temperature occurred on the wound location at all presenting times. Especially, at time 30 seconds, the maximum temperature in BSS and OVD were 49.2°C and 41.7°C, respectively. The maximum temperature difference between BSS and OVD, on the wound location at time 10, 20, and 30 seconds were 4.0°C, 6.2°C, and 7.5°C, respectively.

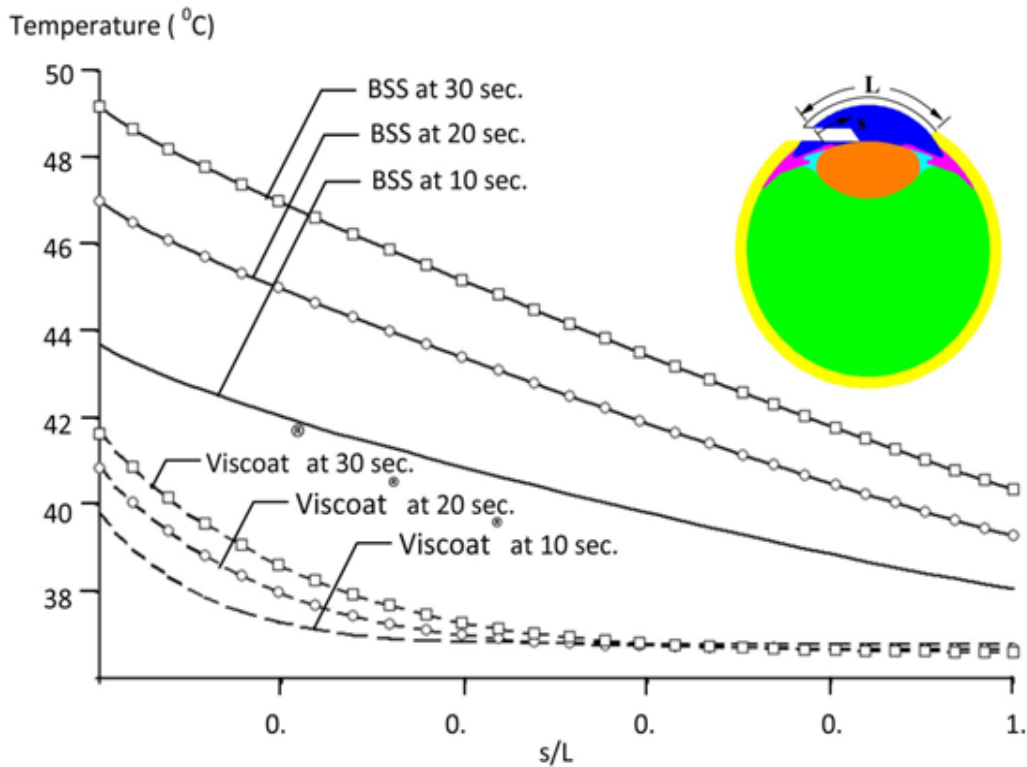


Fig. 4 Plot of temperature vs. s/L ratio (s : varies from 0 to L ; L : maximum length is 11.48 mm.) at the time of 30 seconds.

Discussion

Numerical approaches using computer fluid dynamics (CFD) is most useful for biomedical studies in various organs including brain [17] and nose [18]. In some earlier numerical studies involving ocular models, the finite difference method was used to solve human eye heat transfer [19, 20]. The temperature rise in the human eye exposed to electromagnetic waves was modeled by the finite different time domain method [21, 22]. Bioheat transfer in human eye was also studied by the boundary element method [23, 24] and finite element method [16, 25-28].

During ophthalmic phacoemulsification operation, the phaco needle produces heat by oscillation as soon as the electric power is applied. In our experiment, the heat flux from the phaco needle without sleeve cover was 1.6 kW/m^2 . When the anterior chamber is fully filled with solution (BSS or OVD), heat from the outer surface of the cornea is conducted to the air at the room temperature.

In the present measurement of the thermal properties of BSS and OVD, the thermal diffusivity in BSS was much greater than that in OVD, that is, approximately 20 times. This indicates that OVD may

adjust its temperature to its surroundings more rapidly than BSS.

Based on the transient heat transfer theory and boundary conditions, the 2D nodeless variable finite element method was applied to predict the transient temperature distribution in the eye chamber during a fully occluded phacoemulsification. For two solutions fully filled in the chamber, transient temperature distributions were computed at the time of 10, 20, and 30 seconds. At 30 seconds, the temperature on the corneal endothelium was elevated at maximum up to 49°C or 42°C in BSS or OVD, respectively. Interesting, the temperature elevation by the phaco needle was lower in OVD than BSS. It is likely that OVD may protect the endothelium against heat better than BSS. The present result correlates well with *in vivo*-rabbit study using thermal camera by Jurowski et al. [29].

It is not certain whether these levels of elevated temperature by the phaco needle may injure the corneal endothelial cells or not. However, our computed temperatures are important for the selection of a solution to reduce the risk of corneal endothelial cell injury.

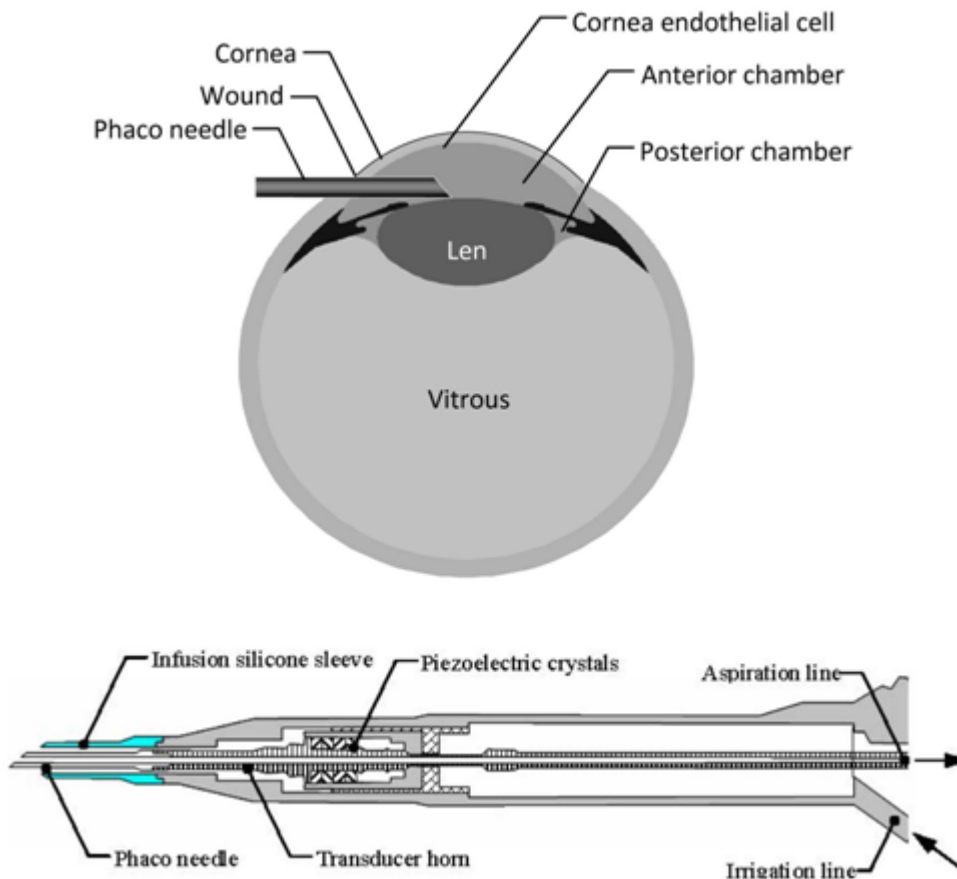


Fig. 5 The structure of the eye where a phaco needle is inserted in the anterior chamber during phacoemulsification (upper) and phaco handpiece components (lower).

In conclusion, the 2D nodeless variable finite element method offers a capability of in-vivo simulation to predict transient temperature response for reducing the risk of thermal-induced blindness during ophthalmic phacoemulsification. The present results may give us a rationale to postulate another mechanism for corneal endothelial cell injury and hand-out the caution of different ophthalmic solution responses to heat. Further investigation of thermal-induced corneal endothelial injury will be crucial for improving the phaco-emulsification safety guideline.

Acknowledgements

The authors acknowledge the National Research Council of Thailand, the Thailand Research Fund (TRF) and Thammasat University for supporting this research work. There is no commerce financial support or any conflict of interest.

Appendix

The structure of eye and a phaco needle inserted during phacoemulsification (Fig. 5).

The piezoelectric crystal is displaced at a certain ultrasonic frequency of 28.5 or 40 kHz depending on the machine. For a thermal aspect rationale, 28.5 kHz tool generates heat less. The ultrasonic frequency of the Millennium® phaco machine (Bausch & Lomb Co, New York, USA) is 28.5 kHz. The oscillation of phaco needle-tip is driven by the attached piezoelectric crystal (transmit by the transducer horn) at variable stroke length with the maximum stroke length of 160 micron [30, 31].

Basic equations for simulation

In general, temperature (T) on the median plane of eye changes in time (t) and is distributed in space (x, y). The transient temperature behavior is described by the heat transfer equation as follows:

$$\rho c \frac{\partial T}{\partial t} = k \frac{\partial^2 T}{\partial x^2} + k \frac{\partial^2 T}{\partial y^2}, \tag{1}$$

where ρ is the density of tissue, c is the specific heat capacity of tissue, and k is the thermal conductivity

coefficient of tissue. The boundary condition is given by specified temperature of T_0 , convection heat transfer, and specified heat flux q_s as follows:

$$T(x,y) = T_0, \tag{2}$$

$$-k \frac{\partial T}{\partial x} n_x - k \frac{\partial T}{\partial y} n_y = h (T_s(x,y) - T_\infty), \tag{3}$$

$$-k \frac{\partial T}{\partial x} n_x - k \frac{\partial T}{\partial y} n_y = q_s, \tag{4}$$

where n_x and n_y are the direction cosines of the vector normal to the surface, h is the convection coefficient, $T_s(x,y)$ is temperature along the boundary, and T_∞ is the surrounding medium temperature.

In the present simulation, we use triangular element (3 nodes and 3 nodeless variables) as shown in Fig. 6.

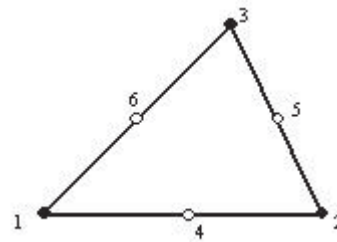


Fig. 6 Nodeless variable element.

Then, its element interpolation functions are as follows:

$$N_i(x,y) = \frac{1}{2A} (a_i + b_i x + c_i y) \quad i = 1, 3 \tag{5}$$

$$N_4 = 4N_1 N_2; \quad N_5 = 4N_2 N_3; \quad N_6 = 4N_1 N_3 \tag{6}$$

In the above Eq. (5), $a_i = x_j y_k - x_k y_j$, $b_i = y_j - y_k$, $c_i = x_k - x_j$ for $i, j, k = 1, 2, 3$, and A is the element area.

The Galerkin approach and the recurrence relations are applied to Eq. (1) leading to the finite element equations in the form:

$$\frac{1}{\Delta t} [C] \{T\}_{n+1} = \left(\frac{1}{\Delta t} [C] - [K] \right) \{T\}_n + \{Q\}_c + \{Q\}_h + \{Q\}_{q_s}, \quad (7)$$

where $[C] = \int_{\Omega} \{N\} \rho c [N] d\Omega$

$$[K] = \int_{\Omega} \left\{ \frac{\partial N}{\partial x} \right\} k \left[\frac{\partial N}{\partial x} \right] d\Omega + \int_{\Omega} \left\{ \frac{\partial N}{\partial y} \right\} k \left[\frac{\partial N}{\partial y} \right] d\Omega + \int_S h \{N\} [N] dA$$

$$\{Q\}_c = \int_S \{N\} k \left(\frac{\partial T}{\partial x} n_x + \frac{\partial T}{\partial y} n_y \right) dS$$

$$\{Q\}_h = \int_S \{N\} h T_s dS$$

$$\{Q\}_{q_s} = \int_S \{N\} q_s dS,$$

and Δt is the time step.

References

- World Health Organization. Programme for the Prevention of Blindness and Deafness. Global Initiative for the Elimination of Avoidable Blindness. WHO/PBL/97.61 1998:1-2.
- Taylor DM, Atlas BF, Romanchuck KG, Stern AL. Pseudophakic bullous keratopathy. *Ophthalmology*. 1983; 90:19.
- Murano N, Ishizaki M, Sato S, Fukuda Y, Takahashi H. Corneal endothelial cell damage by free radicals associated with ultrasound oscillation. *Arch Ophthalmol*. 2008; 126: 816-21.
- Takahashi H. Free radical development in phacoemulsification cataract surgery. *J Nippon Med School*. 2005; 72: 4-12.
- Robert HO, Injev VP. Thermal study of bare tips with various system parameters and incision sizes. *J Cataract Refract Surg*. 2006; 32: 867-72.
- Olson MD, Miller KM. In-air thermal imaging comparison of Legacy AdvanTec, Millennium, and Sovereign WhiteStar phacoemulsification systems. *J Cataract Refract Surg*. 2005; 31: 1640-47.
- Mackool RJ, Sirota MA. Thermal comparison of the AdvanTec Legacy, Sovereign WhiteStar, and Millennium phacoemulsification systems. *J Cataract Refract Surg*. 2005; 31:812-7.
- Aron DR, Vasudev K. Thermal imaging study comparing phacoemulsification with the sovereign with white star system to the legacy with advantec and neosonix system. *Am J Ophthalmol*. 2009; 141:322.
- Mencucci R, Ambrosini S, Vannelli GB, Menchini. Ultrasound thermal damage to rabbit corneas after simulated phacoemulsification. *J Cataract Refract Surg*. 2005; 31:2180-6.
- Limtrakarn W. Nodeless finite element method for 2D potential flow problems. *Thammasat Intern J SciTechnol*. 2005; 10: 41-7.
- Incropera FP, Dewitt DP. *Fundamentals of Heat and Mass Transfer*, 4th Edition. New York:John Wiley & Sons, 1996.
- Zienkiewicz OC, Taylor RL. *Finite Element Method*, 5th Edition. Butterworth:Heinemann, Woburn, 2000.
- Dechaumphai P. *Finite Element Method in Engineering*, Third Ed. Bangkok:Chulalongkorn University Press, 2004.
- Limtrakarn W, Reepolmaha S, Uthaisang W. Application of 3D finite element method to reduce cornea damage during ophthalmic phacoemulsification, *NRCT Res Rep*. 2007.
- Tasman W, Jaeger EA. *Duane's Clinical Ophthalmology*. Baltimore:Lippincott Williams & Wilkins, 2007.
- Cicekli U. Computational model for heat transfer in the human eye using the finite element method. MSc Thesis. Department of Civil and Environmental Engineering, Louisiana State University, 2003.
- Niimi H, Komai Y, Yamaguchi S, Seki J. Microembolic flow disturbances in the cerebral microvasculature with an arcadal network: a numerical simulation. *Clin Hemorheol Microcirc*. 2006; 34: 247-55.
- Zubair A, Riazuddin VN, Abdullah MZ, Ismail R,

- Shuaib IL, Hamid SA, et al. Airflow inside the nasal cavity: visualization using computational fluid dynamics. *Asian Biomed.* 2010; 4:657-61.
19. Lagendijk JJW. [A mathematical model to calculate temperature distributions in human and rabbit eyes during hyperthermic treatment.](#) *Phys Med Biol.* 1982; 27:1301-11.
 20. Okuno T. Thermal effect of infra-red radiation on the eye: a study based on a model. *Ann Occupational Hygiene.* 1995; 35:1-12.
 21. Hirata A, Matsuyama S, Shiozawa T. Temperature rises in the human eye exposure to EM wave in the frequency range 0.6-6 GHz. *IEEE Trans Electromag Compat.* 2000; 42: 386-93.
 22. Hirata A. Temperature increase in human eyes due to near-field and far-field exposures at 900 MHz, 1.5 GHz and 1.9 GHz. *IEEE Trans Electromag Compat.* 2005; 47: 68-76.
 23. Poljak D, Peratta A, Brebbia CA. The boundary-element electromagnetic-thermal analysis of human exposure to base station antennas radiation. *Eng Anal Boundary Elements.* 2004; 28: 763-70.
 24. Ooi EH, Ang WT, Ng EYK. Bioheat transfer in the human eye: a boundary element approach. *Eng Anal Boundary Elements.* 2007; 31:494-500.
 25. Scott JA. [A finite element model of heat transport in the human eye.](#) *Phys Med Biol.* 1988; 33: 227-41.
 26. Heys JJ, Barocas VH. A Boussinesq model of natural convection in the human eye and the formation of krukenberg's spindle. *Ann Biomed Eng.* 2002; 30: 392-401.
 27. [Ng EYK, Ooi EH. FEM simulation of the eye structure with bioheat analysis.](#) *Comput Meth Progr Biomed.* 2006; 82:268-76.
 28. Ooi EH, Ng EYK. Simulation of aqueous humor hydrodynamics in human eye heat transfer. *Comput Meth Progr Biomed.* 2008; 38:252-62.
 29. Jurowski P, Gos R, Owczarek G, Gralewicz GZ. Corneal endothelial cells' protection against thermal injury: influence of ophthalmic viscoelastic substances in experimental study on rabbits. *Eur J Ophthalmol.* 2005; 15: 674-9.
 30. Seibel BS. *Phacodynamics-Mastering the Tools and Techniques of Phacoemulsification Surgery*, Forth Edition. Thorofare:Slack Incorporated. 2005.
 31. Reepolmaha S, Tangsirichaipong A. Comparative study of stroke length between Millennium and Infinity by photographic method. *Abstr 25th Congr Eur Soc Cataract Refract Surgeons, Stockholm, 2007:123.*